

Evolution of the quasiparticle spectral function in cuprates

S. Misra, R. Gatt, T. Schmauder, Andrey V. Chubukov and M. Onellion*
Department of Physics, University of Wisconsin, Madison, WI 53706

M. Zacchigna, I. Vobornik, F. Zwick, M. Grioni and G. Margaritondo
École Polytechnique Fédérale Lausanne, CH-1015 Lausanne, Switzerland

C. Quitmann
Experimentalphysik I, Universität Dortmund, D-44221 Dortmund, Germany

C. Kendziora
Naval Research Laboratory, Washington D.C.
 (May 5, 2019)

We analyzed photoemission data for several doping levels of the $Bi_2Sr_2CaCu_2O_{8+x}$ compounds, ranging from overdoped to underdoped. We show that the high frequency part of the spectra near $(0, \pi)$ can be described by Fermi liquid theory in the overdoped regime, but exhibits a non-Fermi liquid behavior in the underdoped regime. We further demonstrate that this novel behavior fits reasonably well to a $1/\sqrt{\omega}$ behavior suggested for systems with strong spin fluctuations.

74.20.Jb

One of the most intriguing characteristics of the cuprates is their qualitative change in electronic properties with doping. These changes have been attributed mostly to the pseudogap that appears in the normal state at frequencies comparable to the superconducting gap. The goal of this communication is to show that in addition to the pseudogap, the high frequency part of photoemission spectra exhibit qualitative changes with decreasing carrier concentration. We argue below that this evolution with doping indicates that the cuprates are near a quantum critical point and exhibit a non-Fermi liquid spectral function for high frequencies.

A series of recent papers have reported that the spectral weight of the quasiparticle peak near the Fermi surface becomes smaller for underdoped samples, and that there is a transfer of spectral weight to the high-frequency part of the spectrum [1]. In this paper, we present a functional analysis of such data. Our main result is that the photoemission intensity $I(\omega)$ undergoes a particular type of crossover behavior with decreasing doping (since energy is $\hbar\omega$, we subsequently refer to the frequency ω). The spectral function changes from a behavior which can be reasonably well described by the Fermi liquid form $I^{-1}(\omega) \propto (\Gamma^2 + \omega^2)$ to a behavior which to good accuracy can be described by a non-Fermi liquid form $I^{-1}(\omega) \propto \sqrt{\omega}$. Such behavior is predicted when the dominant effect of quasiparticle decay is the interaction with overdamped spin fluctuations [2].

We begin by reviewing the theoretical aspects of the problem. In the sudden approximation, the photoemission intensity at a given momentum k is given by $I_k(\omega) = A_k(\omega)n(\omega)$ where $A_k(\omega) = (1/\pi)ImG_k(\omega)$ is the quasiparticle spectral function, and $n(\omega)$ is the Fermi function which selects states occupied by electrons. Fermi liquid theory predicts that, regardless of how strong the interaction is, the single-particle Green's function at low frequencies has the form

$$G_k(\omega) = \frac{Z}{(\omega - (\epsilon_k - \epsilon_F) + i\omega|\omega|/\Gamma)}, \quad (1)$$

where ϵ_F is the Fermi energy. For momenta near the Fermi surface, i.e., at small $\epsilon_k - \epsilon_F$, the spectral function which emerges from $G_k(\omega)$ possesses a quasiparticle peak at $\omega = \epsilon_k - \epsilon_F$; the width of the peak decreases as $(\epsilon_k - \epsilon_F)^2$ with the approach of the Fermi surface. At the Fermi-surface, the quasiparticle peak transforms into a δ -function for $\omega = 0$, while for frequencies $\omega \leq \Gamma$, $A_k(\omega)$ takes the form $A_k^{-1}(\omega) \propto (\omega^2 + \Gamma^2)$. The inverse proportionality to ω^2 at low frequencies is a fundamental property of Fermi liquids which does not depend on details of the quasiparticle interaction. However, Γ , which serves as the upper frequency cutoff for this universal behavior, is model dependent. When the Fermi system is far from any instability, Γ is of the order as ϵ_F , which is typically the upper cutoff for a low energy description (i.e., expansion in powers of ω). This changes if the system is close to a quantum critical point where it undergoes a spontaneous symmetry breaking. In this situation, $\Gamma \ll \epsilon_F$ and Γ scales with the distance from the critical point. For $\omega \ll \Gamma$, the system still possesses Fermi liquid behavior- i.e., $A_k^{-1}(\omega) \propto (\omega^2 + \Gamma^2)$. However, for $\Gamma \ll \omega \ll \epsilon_F$ the system crosses over into the region which is in the basin of attraction of the quantum critical point. In this region the system behavior is governed by critical fluctuations. These fluctuations impose a novel

frequency dependence of the spectral function up to frequencies comparable to the Fermi energy. It is essential that this picture survives even if the system trajectory in the phase space of parameters slightly bypasses the quantum critical point (e.g., the actual transition into the symmetry breaking state can be a weak first order transition or involve an intermediate phase) or the system possesses a low-energy crossover from one type of critical behavior to that associated with small but relevant perturbations around the quantum critical point (in cuprates this may be due to a Fermi surface evolution very near the magnetic instability). These effects reduce the range of Fermi-liquid behavior to even smaller frequencies, but they do not modify the behavior at $\omega > \Gamma$ as long as Γ remains the largest energy scale associated with instability.

In recent years there have been a number of suggestions for possible quantum critical points in the cuprates [3]. In our opinion, the most plausible candidate is the instability point towards antiferromagnetism. The system approaches this critical point as the carrier concentration decreases, and the system is antiferromagnetic at half-filling. The quantitative measure of closeness to a magnetic transition is the spin correlation length, ξ . When ξ is large enough, the system behavior is predominantly critical over a wide frequency range. As ξ clearly increases with decreasing doping, the range of critical behavior also increases.

Recently, one of us (AC) considered the interaction between fermions and overdamped spin fluctuations and found that $\Gamma \sim \omega_{sf}$ where $\omega_{sf} \propto \xi^{-2}$ is a typical spin-fluctuation scale [2]. More specifically, the fermionic Green's function along some portion of the Fermi surface near $(0, \pi)$ and related points was shown to have the form

$$G^{-1}(\omega) \propto \frac{1}{Z} \frac{2\omega}{1 + \sqrt{1 - i|\omega|/\omega_{sf}}}, \quad (2)$$

where $Z \propto \xi^{-1}$. At small frequencies, $\omega \leq \omega_{sf}$, this Green's function has a conventional Fermi-liquid form $G^{-1}(\omega) \propto (\omega + i\omega|\omega|/(4\omega_{sf}))$. At higher frequencies, however, the Fermi-liquid form crosses over to a region of novel frequency dependence- $G(\omega) \propto Ae^{-i\pi/4}|\omega|^{-1/2}\text{sgn}\omega$, where $A = Z\omega_{sf}^{-1/2}$. As A is independent of ξ , it remains finite when $\xi \rightarrow \infty$, as it should for quantum critical behavior. One can probe this behavior at finite ξ for $|\omega| \gg \omega_{sf}$. Values of ω_{sf} for various dopings have been extracted from available NMR data [4]. The NMR data indicate that ω_{sf} (at a given T) increases with doping and remains $\sim 20 - 30\text{meV}$ (i.e., small compared to ϵ_F) for overdoped cuprates. From this perspective, some features of the crossover to $\sqrt{\omega}$ behavior should be observed even in the data for overdoped cuprates.

The tendency towards quantum critical behavior is much less pronounced near the Fermi surface crossing along the zone diagonal ($\langle\pi, \pi\rangle$ direction). Here, calculations show that the analog of ω_{sf} remains finite for $\xi \rightarrow \infty$ with a value comparable to ϵ_F . The system is therefore in the moderate coupling regime; $A(\omega)$ at intermediate ω should display a frequency dependence which is intermediate between quantum-critical and Fermi liquid forms.

We now turn to the analysis of the photoemission data. The photoemission data were measured using angle-resolved photoemission equipment at the Wisconsin Synchrotron Radiation Center and at École Polytechnique Fédérale Lausanne; the equipment details are provided in Ref. [5]. Samples were fabricated as reported in the literature [6], and were transferred via a load-lock system so as to retain the oxygen content. The data were taken at a temperature well into the normal state (typically 200K for underdoped samples, 100K for overdoped samples), and above the temperature, T^* , below which a pseudogap would be observed. In addition, we analyzed the data from Ref. [7] and found our conclusions to be consistent with that report. Altogether, we analyzed data on seven doping levels, including overdoped ($T_C \approx 52\text{K}$, 65K and 75K), optimally doped ($T_C \approx 90\text{K}$), and underdoped ($T_C \approx 60\text{K}$ and 30K), in addition to analyzing underdoped data ($T_C \approx 85\text{K}$) from Ref. [7]. The details of all samples and doping levels are reported elsewhere [8].

We analyzed the photoemission data using seven different techniques, including fitting using the chi-squared criterion (with four different background subtraction methods), the Kolmogorov-Smirnov criterion, the ratio of data at different binding energies, and the inverse of the data. We provide a complete, detailed discussion of these analysis methods elsewhere [8]. All seven methods led to the same conclusion, that there is a qualitative change in the nature of the spectral function with doping. Due to space limitations, we emphasize two of these methods in this report.

We first summarize our results. For overdoped cuprates near $(0, \pi)$, we found that the data below $\sim 250\text{meV}$ (the exact value depends somewhat on the background subtraction method employed) were consistent with the Fermi liquid Green's function (Eq. 1) and were inconsistent with the Green's function of Eq. 2. For higher frequencies, however, we found some evidence for a crossover to quantum-critical behavior. For overdoped cuprates along the $\langle\pi, \pi\rangle$ direction, the data were also consistent with Eq. 1. For underdoped samples near $(0, \pi)$, we found that the data were consistent with Eq. 2, and were inconsistent with a Fermi liquid Green's function over the entire frequency range studied. In the $\langle\pi, \pi\rangle$ direction, the data are fit equally well by either the Fermi liquid or the non-Fermi-liquid spectral functions.

We now discuss in more detail how we actually fitted the data. We began by checking whether the finite energy resolution of our equipment significantly modified the functional forms of either Eqs. 1 or 2. To do this, we generated spectra by convoluting each of the two theoretical spectral functions with the experimental resolution function, and subsequently fitted the results using the unbroadened functional forms of Eqs. 1 and 2. We found that the finite energy resolution of the electron analyzer has only a small impact on the analyses and could be almost fully absorbed into small renormalization of the input parameters, ω_{sf} and Γ .

In our first method, we took special care in dealing with the background. The key assumption we made is that photoemission spectra for wavevectors far from the Fermi surface are indistinguishable from the background. Analyzing the data in these k -ranges, we observe that they are nearly frequency independent over a relatively wide frequency range. The insets of Fig. 1 illustrate this situation (the flat regions are indicated by arrows). We further assumed that the flat background is independent of k , i.e., it remains the same near the Fermi surface. We then eliminate this background by replotting the data in the form $R(\omega) = ((I(\omega) - I(\omega_{max})) / (I(\omega_{min}) - I(\omega)))$ where ω_{min} and ω_{max} are the lower and upper boundaries of the region where the background is independent of frequency. Plotting the data in this form additionally allows us to eliminate the overall factor in the intensity. Finally, we fit $R(\omega)$ by Fermi-liquid and spin-fluctuation forms using ω_{sf} and Γ as adjustable parameters and check which form works better.

Applying this method to experimental data, we obtain the results presented in Fig. 1. The actual spectra from which the fits were obtained are the upper curves in the insets of each part of Fig. 1. We include three sets of data- oxygen overdoped material ($T_C \approx 65K$), oxygen underdoped material ($T_C \approx 30K$ and $60K$), and Dy-doped underdoped material ($T_C \approx 85K$) from Ref. [7]. The spectra analyzed are those for the k -points closest to the Fermi surface. For overdoped samples near the $(0, \pi)$ point, the data consistently yield a better fit for Eq. 1. Along the $\langle \pi, \pi \rangle$ direction, the data are also fit better by Eq. 1, although the error bars are more significant. For underdoped materials near the $(0, \pi)$ point, the spectral function from Eq. 2 yields a much better fit than that of a Fermi liquid. Furthermore, we consistently obtain a spin fluctuation energy of 30- 40 meV , which is a bit larger than, but still comparable to, the $\omega_{sf} \sim 10 - 20meV$ extracted from NMR. Along the $\langle \pi, \pi \rangle$ direction, both spectral functions fit the data equally well, thus we cannot judge which form works better.

In the second method of analysis, we assumed that the background is independent on k over the whole frequency range studied in photoemission. After making this assumption, we subtracted the data for k -values far away from the Fermi surface from the data near the $(0, \pi)$ point, inverted the subtracted data, and fitted the results to both Fermi liquid (ω^2) and $\sqrt{\omega}$ forms. This method allowed us to fit the data over a wider frequency range than the first one. The results are shown in Fig. 2. The results provide additional insights to the results in Fig. 1. For overdoped samples, we find that the data are fit best by a quadratic (Fermi liquid) form for binding energies up to $\sim 250meV$, and by a $\sqrt{\omega}$ form for higher binding energies. The exact binding energy of the crossover depends somewhat on the background subtraction method employed. For underdoped samples, the data in Fig. 2 are better fit by a $\sqrt{\omega}$ form for the entire binding energy range above $\sim 100meV$. We also performed the same analysis for the data taken near the Fermi surface crossing along the $\langle \pi, \pi \rangle$ direction (not shown in Fig. 2). For both overdoped and underdoped samples, the Fermi liquid and non-Fermi liquid forms fit the data equally well. As a consequence, it is difficult to assess which form works better in the along the $\langle \pi, \pi \rangle$ direction for any doping level.

In summary, theory predicts that when doping decreases, the Fermi-liquid form of the spectral function near $(0, \pi)$ exists in progressively smaller range of low frequencies, while at higher frequencies the spectral function crosses over to a novel frequency dependence, $A^{-1}(\omega) \propto \sqrt{\omega}$, associated with the closeness to an antiferromagnetic quantum critical point. Experimentally, we have measured and analyzed the high frequency part of the photoemission data for BSCCO-2212 materials and its variation with doping. We found that the data near $(0, \pi)$ for underdoped cuprates agrees well with the spin-fluctuation form of the spectral function, Eq. 2. For the frequency range we used, it yields a non-Fermi liquid form $A^{-1}(\omega) \propto \sqrt{|\omega|}$. In contrast, the data for overdoped cuprates is well-fitted by the Fermi liquid form $A^{-1}(\omega) \propto (\omega^2 + \Gamma^2)$ over a substantial frequency range (up to $\sim 250meV$). At larger frequencies, we found some evidence for crossover to $1/\sqrt{|\omega|}$ behavior. Overdoped cuprates in the $\langle \pi, \pi \rangle$ direction exhibit Fermi liquid behavior. Neither analysis method yields conclusive results for underdoped cuprates in the $\langle \pi, \pi \rangle$ direction.

Financial support was provided by the NSF DMR-9629839 (AC), DMR-9632527 (SM, RG, MO), ONR through NRL (CK), Fonds National Suisse (EPFL, TS), and Deutsche Forschungsgemeinschaft (CQ). (SM) acknowledges support from a Hilddale Fellowship.

* corresponding author: M. Onellion

email: onellion@comb.physics.wisc.edu

- [1] H. Ding *et al.*, Nature **382**, 51 (1996); Z.-X. Shen and J.R. Schrieffer, Phys. Rev. Lett. . **78**, 1771 (1997); M. Norman *et al.*, Nature **392**, 157 (1998).
- [2] A. Chubukov, Phys. Rev. B **52**, R3840 (1995) and cond-mat/9709221; A.Millis, Phys. Rev. B **45**, 13047 (1995); A.V. Chubukov and J. Schmalian, Phys. Rev. B to appear.
- [3] A. Chubukov, S. Sachdev and J. Ye, Phys. Rev. B **49**, 11919 (1994); R. Laughlin, Phys. Rev. Lett. **79**, 1726 (1997) and unpublished; S.C. Zhang, Science **285**, 1089 (1997); A.V. Chubukov, D.K. Morr and K. Shakhnovich, Phil. Mag. B **74**, 563 (1996).
- [4] V. Barzykin and D. Pines, *ibid*, **52**, 13585 (1995).
- [5] Jian Ma *et al.*, Phys. Rev. B **51** 3832, 9271 (1995). I. Vobornik *et al.*, Surf. Sci., in press (1998).
- [6] C. Kendziora *et al.*, Physica C **257**, 74 (1996).
- [7] D.S. Marshall *et al.*, Phys. Rev. Lett. **76**, 4841 (1996).
- [8] S. Misra *et al.*, unpublished.

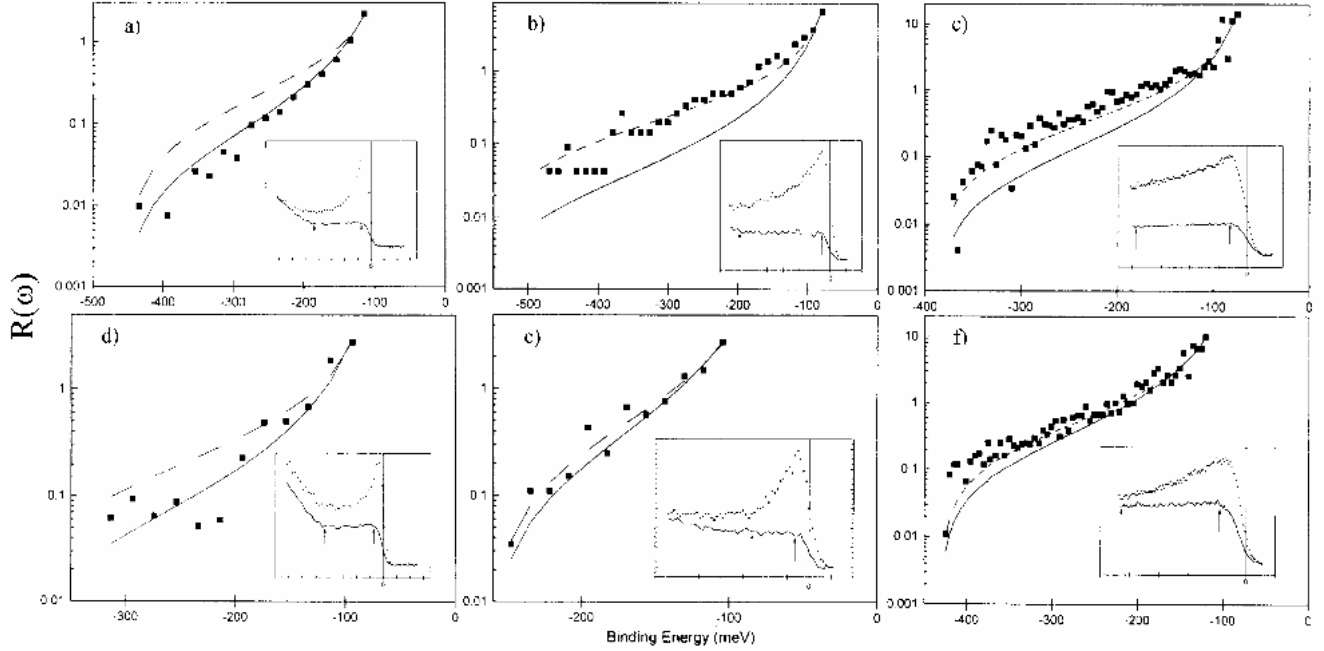


FIG. 1. The fits of the normalized photoemission intensity $R(\omega)$ by the Fermi-liquid frequency dependence, Eq. 1 (dotted line), and by the spin-fluctuation form, Eq. 2 (solid line). The horizontal axis is the electron binding energy from 0 (the Fermi energy) and the hash marks 100 meV apart. The vertical axis is $R(\omega)$ on a logarithmic scale. Figs. (a)-(c) are fits to the data near the $(0, \pi)$ point including: (a) oxygen underdoped, $T_C \approx 60K$ material, (b) Dy-underdoped, $T_C \approx 85K$ material from Ref. [7], and (c) oxygen overdoped, $T_C \approx 65K$ material. Figs (d)-(f) are fits to the data near the Fermi surface crossing in the (π, π) direction, including: (d) oxygen underdoped, $T_C \approx 30K$ material, (e) Dy- underdoped, $T_C \approx 85K$ from Ref. [7] (same as in Fig. (b)), and (f) oxygen overdoped, $T_C \approx 65K$ material. Insets to the figures show angle-resolved photoemission spectra taken near the Fermi surface (upper spectra) and far away from the Fermi surface (lower spectra). The horizontal axis is the electron binding energy, from 0 (Fermi energy) and the hash marks are 100 meV apart. The arrows indicate the frequency range for which the spectra far away from the Fermi surface are frequency independent. This is the range over which we fitted $R(\omega)$.

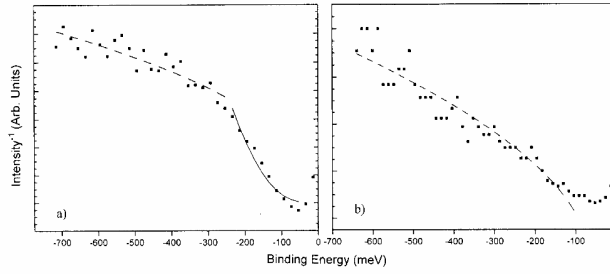


FIG. 2. Results of the second analysis method of fitting the data. We subtracted the data far away from the Fermi surface (which we identify with the background) from the data taken near the Fermi surface crossing near the $(0, \pi)$ point for all k -values and inverted the difference. We then fitted the inverse intensity by the Fermi-liquid, ω^2 form, (dotted line) and the $\sqrt{\omega}$ form (solid line), which is the high-frequency limit of the spin-fluctuation form (Eq. 2). Figs (a) and (b) are the fits for oxygen overdoped, $T_C \approx 65K$ material and oxygen underdoped, $T_C \approx 60K$ material, respectively. Observe that the ω^2 form does not fit the data for underdoped sample at all. For overdoped sample, the ω^2 form fits data for binding energy up to $\sim 250meV$, above which there is a crossover to the $\sqrt{\omega}$ dependence.